

# N-Linked Peptidoresorc[4]arene-Based Receptors as Noncompetitive Inhibitors for $\alpha$ -Chymotrypsin

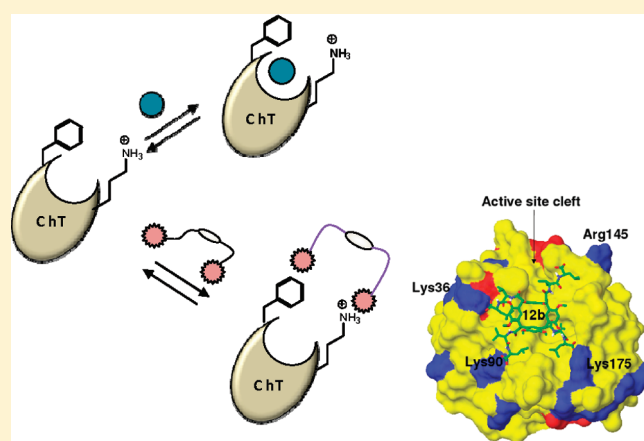
Ilaria D'Acquarica,<sup>†</sup> Antonella Cerreto,<sup>†</sup> Giuliano Delle Monache,<sup>†</sup> Fabiana Subrizi,<sup>†</sup> Alberto Boffi,<sup>‡</sup> Andrea Tafi,<sup>§</sup> Stefano Forli,<sup>§,||</sup> and Bruno Botta<sup>\*,†</sup>

<sup>†</sup>Dipartimento di Chimica e Tecnologie del Farmaco and <sup>‡</sup>Dipartimento di Scienze Biochimiche, Sapienza Università di Roma, P. le Aldo Moro 5, 00185 Roma, Italy

<sup>§</sup>Dipartimento Farmaco Chimico Tecnologico, Università degli Studi di Siena, Via Aldo Moro, 53100 Siena, Italy

 Supporting Information

**ABSTRACT:** This paper deals with the design, synthesis, and evaluation of a new series of receptors for protein surface recognition. The design of these agents is based around the attachment of four constrained dipeptide chains onto a central resorc[4]arene scaffold. By varying the sequence, nature, and stereochemistry of the chains we prepared anionically functionalized N-linked peptidoresorc[4]arenes **12**, **13**, and **17** by Pd/C-catalyzed hydrogenation of the corresponding benzyl esters **10**, **11**, and **16**. From this family of receptors we have identified noncompetitive inhibitors of  $\alpha$ -chymotrypsin (ChT), which function by binding to the surface of the enzyme in the neighborhood of the active site cleft ( $K_i$  values ranging from  $12.4 \pm 5.1 \mu\text{M}$  for free carboxylic acid (+)-**12b** to  $0.76 \pm 0.14 \mu\text{M}$  for benzyl ester (–)-**16a**). For anionically functionalized receptors **12**, **13**, and **17** the ChT inhibition is based essentially on electrostatic interaction, and the bound enzyme can be released from the resorc[4]arene surface by increasing the ionic strength, with its activity almost completely restored. For receptors with terminal benzyl ester groups (**10** and **16**) a hydrophobic network can be suggested.



## INTRODUCTION

Because of their key role in a number of biological processes, protein–protein interactions (PPI)<sup>1</sup> are attractive and important targets for the design of novel therapeutics. Synthetic receptors targeted at protein surfaces provide an alternative paradigm to active site inhibition for the disruption of such interactions.<sup>2</sup> Covalent modification of a protein with a polymer offers the opportunity of irreversibly modifying its biological activity.<sup>3</sup> On the other hand, noncovalent interactions of proteomimetics, i.e., molecules that mimic the structure and function of extended regions of protein surfaces, offer the possibility of reversible binding and modulation of the protein function itself. Among these synthetic receptors, small molecules,<sup>4</sup>  $\alpha$ -helix mimetics based on terphenyl or terephthalamide scaffolds,<sup>5</sup> multidentate ligands,<sup>6</sup> functionalized nanoparticle scaffolds,<sup>7</sup> and macrocyclic systems, such as porphyrins<sup>8</sup> and calixarenes,<sup>9</sup> have been successfully used as protein inhibitors. We have recently introduced a new class of resorc[4]arenes based on the attachment of four constrained dipeptide chains onto a central macrocyclic scaffold.<sup>10a,b</sup> The flexible conformation and the occurrence of multiple contacts by a variable peptide sequence offered by the system appeared theoretically adapt for binding the convex and solvent

exposed surface of proteins.<sup>11</sup> Moreover, a further approach to recognition was predicted in the insertion of charged hydrophilic carboxylate groups<sup>12</sup> or lipophilic benzyl groups in the terminal amino acid, which might contact complementary residues across the surface of the protein, by electrostatic or hydrophobic interactions, respectively. With the aim of proposing our N-linked peptidoresorc[4]arenes as synthetic receptors for protein surface binding, we therefore prepared anionically functionalized macrocycles by the ex novo synthesis of N-linked peptidoresorc[4]arene benzyl esters **10**, **11**, and **16**, which were in turn hydrolyzed to the corresponding free carboxylic acids **12**, **13**, and **17**. In preliminary studies, we tested the effective interaction between **12** and human serum albumin (HSA), the most common serum protein. Afterward, we explored the binding and the concomitant inhibition of  $\alpha$ -chymotrypsin (ChT), a popular substrate for these experiments,<sup>7,12</sup> which was shown to be inhibited by a specific family of calix[4]arene receptors.<sup>9b,d</sup>

Received: January 7, 2011

Published: May 02, 2011

## RESULTS AND DISCUSSION

**Receptors Design and Synthesis.** An important class of protein surface receptors based on the attachment of four cyclic peptides to a calix[4]arene scaffold was developed by Hamilton and targeted to the serine protease ChT.<sup>9b</sup> Moving from Hamilton's results, we performed preliminary molecular modeling studies suggesting the design of tetra-anionically functionalized receptors that might target the predominantly cationic region of ChT surrounding the active site. We have previously functionalized resorc[4]arene octamethyl ethers at the feet with valine units<sup>10c</sup> and later exploited their capability of enantiodiscriminating amino acidic guests in the gas phase by mass spectrometry. Afterward, we moved to design valyl-leucine and leucyl-valine peptidoresorc[4]arenes<sup>10a,b</sup> inspired by the evidence that *N*- or *C*-linked peptides endow calixarenes with novel properties, such as recognition of protein surfaces and carbohydrates, formation of stable inclusion complexes, and self-assembly phenomena. Resorc[4]arene core in the *cone* conformation was chosen for its high flexibility and for the presence of four *all-cis* substituents that could preorganize the peptide chain on the same side of the scaffold.

Following the scheme of our previous work,<sup>10a</sup> resorc[4]arene octamethyl ether tetraester **1** (Figure 1), obtained as previously

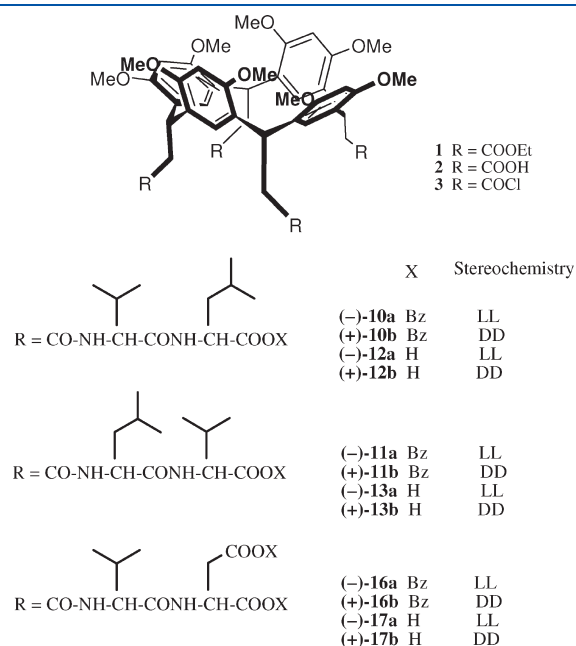
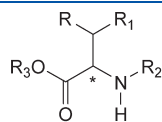


**Figure 1.** *N*-Linked peptidoresorc[4]arene benzyl esters (**10**, **11**, and **16**) and free acids (**12**, **13**, and **17**).



- 4a** R = R<sub>1</sub> = CH<sub>3</sub>, R<sub>2</sub> = BOC, R<sub>3</sub> = H, \* = L  
**5a** R = (CH<sub>3</sub>)<sub>2</sub>CH, R<sub>1</sub> = H, R<sub>2</sub> = H-*p*-toluenesulfonic acid, R<sub>3</sub> = Bz, \* = L  
**7a** R = (CH<sub>3</sub>)<sub>2</sub>CH, R<sub>1</sub> = H, R<sub>2</sub> = BOC, R<sub>3</sub> = H, \* = L  
**8a** R = R<sub>1</sub> = CH<sub>3</sub>, R<sub>2</sub> = H-*p*-toluenesulfonic acid, R<sub>3</sub> = Bz, \* = L  
**14a** R = COOBz, R<sub>1</sub> = H, R<sub>2</sub> = H-*p*-toluenesulfonic acid, R<sub>3</sub> = Bz, \* = L  
**4b** R = R<sub>1</sub> = CH<sub>3</sub>, R<sub>2</sub> = BOC, R<sub>3</sub> = H, \* = D  
**5b** R = (CH<sub>3</sub>)<sub>2</sub>CH, R<sub>1</sub> = H, R<sub>2</sub> = H-trifluoroacetic acid, R<sub>3</sub> = Bz, \* = D  
**7b** R = (CH<sub>3</sub>)<sub>2</sub>CH, R<sub>1</sub> = H, R<sub>2</sub> = BOC, R<sub>3</sub> = H, \* = D  
**8b** R = R<sub>1</sub> = CH<sub>3</sub>, R<sub>2</sub> = H-trifluoroacetic acid, R<sub>3</sub> = Bz, \* = D  
**14b** R = COOBz, R<sub>1</sub> = H, R<sub>2</sub> = H-trifluoroacetic acid, R<sub>3</sub> = Bz, \* = D

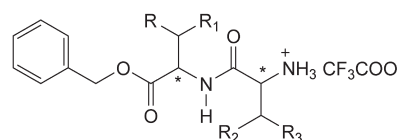
**Figure 2.** Building blocks of the dipeptide chains.

described,<sup>13</sup> was hydrolyzed to tetracarboxylic acid **2** and subsequently treated with thionyl chloride in dry benzene, affording the corresponding acid chloride derivative **3** in quantitative yield.

For the preparation of *L*-valyl-*L*-leucine benzyl ester (**6a**, Figure 2), commercial *N*-Boc-*L*-valine **4a** was coupled with *L*-leucine benzyl ester *p*-toluenesulfonate **5a** in the presence of HOBT and triethylamine to afford *N*-Boc-*L*-valyl-*L*-leucine benzyl ester, which after deprotection with TFA/DCM, gave the dipeptide **6a** as TFA salt. Analogously, *L*-leucyl-*L*-valine benzyl ester **9a**, as TFA salt, was prepared starting from commercial *N*-Boc-*L*-leucine **7a** and *L*-valine benzyl ester *p*-toluenesulfonate **8a**. In both cases, the overall yield was about 85%. The same peptide coupling procedure was applied to the *DD*-dipeptides series: *D*-valyl-*D*-leucine benzyl ester **6b** and *D*-leucyl-*D*-valine benzyl ester **9b**, TFA salts, were obtained with comparable yields, starting from the pairs **4b/5b** and **7b/8b**, respectively. Notably, because **5b** and **8b** were not easily commercially available, they were ad hoc synthesized as TFA salts. The overall yields of the dipeptides were about 80%.

The four **6a**, **6b**, **9a**, and **9b** dipeptides were conjugated individually with macrocycle **3** as follows: DIPEA was added under nitrogen atmosphere to a solution of **3** in dry THF, and the reaction mixture was stirred at room temperature; after the addition of the proper dipeptide benzyl ester in THF, the mixture was refluxed for 1 h. Standard purification gave, in 65–75% yields, the four *N*-linked peptidoresorc[4]arenes benzyl esters **10a**, **10b**, **11a**, and **11b** (Figure 1), which in turn, by hydrogenation with 10% Pd/C, afforded the free carboxylic acids **12a**, **12b**, **13a**, and **13b** (Figure 1). After the positive experimental results of the binding between **12** and HSA (vide infra), four more compounds were synthesized, aiming at doubling the number of terminal functional groups, either for a lipophilic or electrostatic interaction with proteins. *L*-Valyl-*L*-aspartic acid dibenzyl ester (**15a**) and *D*-valyl-*D*-aspartic acid dibenzyl ester (**15b**) were thus prepared by the usual procedure, starting from the proper commercial *N*-Boc-valine (**4a** or **4b**) and the proper aspartic acid dibenzyl ester (commercial **14a** or ad hoc synthesized **14b**). The dibenzylated peptidoresorc[4]arenes **16a** and **16b**, obtained by the coupling with **3** of **15a** and **15b**, respectively, finally gave the corresponding free dicarboxylic acids **17a** and **17b** by Pd/C hydrogenation in quantitative yields. All of the new compounds were structurally confirmed by NMR spectroscopy (see Tables 1S–3S in the Supporting Information) and electrospray ionization high-resolution mass spectrometry (ESI-HRMS, see the Supporting Information for a collection of spectra), as well as by the optical rotation values (see Table 1).

**NMR Analysis of *N*-Linked Peptidoresorc[4]arenes.** As noticed in our previous paper,<sup>10a</sup> for the presence of chiral centers in the side chains, the four symmetry planes (*C*<sub>4v</sub>) of the starting



- 6a** R = (CH<sub>3</sub>)<sub>2</sub>CH, R<sub>1</sub> = H, R<sub>2</sub> = R<sub>3</sub> = CH<sub>3</sub>, \*\* = L,L  
**9a** R = R<sub>1</sub> = CH<sub>3</sub>, R<sub>2</sub> = (CH<sub>3</sub>)<sub>2</sub>CH, R<sub>3</sub> = H, \*\* = L,L  
**15a** R = COOBz, R<sub>1</sub> = H, R<sub>2</sub> = R<sub>3</sub> = CH<sub>3</sub>, \*\* = L,L  
**6b** R = (CH<sub>3</sub>)<sub>2</sub>CH, R<sub>1</sub> = H, R<sub>2</sub> = R<sub>3</sub> = CH<sub>3</sub>, \*\* = D,D  
**9b** R = R<sub>1</sub> = CH<sub>3</sub>, R<sub>2</sub> = (CH<sub>3</sub>)<sub>2</sub>CH, R<sub>3</sub> = H, \*\* = D,D  
**15b** R = COOBz, R<sub>1</sub> = H, R<sub>2</sub> = R<sub>3</sub> = CH<sub>3</sub>, \*\* = D,D

Table 1. Physical Properties of Chiral *N*-Linked Peptidioresorc[4]arenes

compd	peptide sequence	ESI-HRMS ( <i>m/z</i> )	mp (°C)	$[\alpha]_D^{20}$ ( <i>c</i> , solvent)
(–)-10a	L-Val-L-Leu-OBz	1043.53604 ( $[M + 2Na]^{2+}$ )	220–221	–80.5 (1.0, CHCl <sub>3</sub> )
(+)-10b	D-Val-D-Leu-OBz	1043.53635 ( $[M + 2Na]^{2+}$ )	221–222	+79.4 (1.0, CHCl <sub>3</sub> )
(–)-11a	L-Leu-L-Val-OBz	1043.53549 ( $[M + 2Na]^{2+}$ )	248–249	–76.7 (0.3, CHCl <sub>3</sub> )
(+)-11b	D-Leu-D-Val-OBz	1043.53656 ( $[M + 2Na]^{2+}$ )	251–252	+75.9 (1.0, CHCl <sub>3</sub> )
(–)-12a	L-Val-L-Leu-OH	566.62079 ( $[M - 4H + Na]^{3-}$ )	212–213	–55.5 (1.0, MeOH)
(+)-12b	D-Val-D-Leu-OH	566.62022 ( $[M - 4H + Na]^{3-}$ )	209–211	+52.5 (1.0, MeOH)
(–)-13a	L-Leu-L-Val-OH	566.62026 ( $[M - 4H + Na]^{3-}$ )	135–136	–49.2 (0.6, MeOH)
(+)-13b	D-Leu-D-Val-OH	566.61975 ( $[M - 4H + Na]^{3-}$ )	135–136	+46.3 (0.7, MeOH)
(–)-16a	L-Val-L-Asp-OBz	1228.01773 ( $[M + 2Na]^{2+}$ )	218–219	–35.7 (0.5, MeOH)
(+)-16b	D-Val-D-Asp-OBz	1228.01416 ( $[M + 2Na]^{2+}$ )	218–219	+35.9 (0.5, MeOH)
(–)-17a	L-Val-L-Asp-OH	843.33097 ( $[M - 2H]^{2-}$ )	201–202 <sup>a</sup>	–18.3 (0.1, MeOH)
(+)-17b	D-Val-D-Asp-OH	843.32839 ( $[M - 2H]^{2-}$ )	203–204 <sup>a</sup>	+17.7 (0.1, MeOH)

<sup>a</sup>With decomposition.

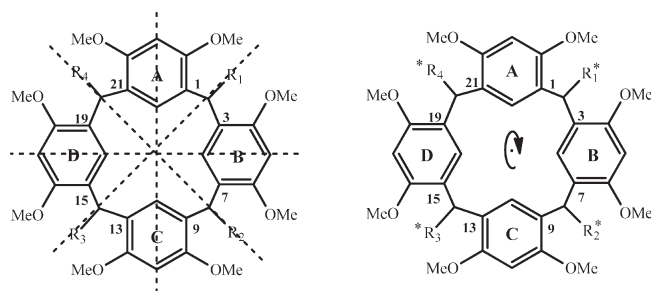


Figure 3. Symmetry in the achiral molecule precursor (left) and the final chiral product (right).

cone conformer **1** are no longer present in the *N*-linked peptide derivatives **10–13**, **16**, and **17** (Figure 3). The planes R1/R3 and R2/R4 contain the chiral centers, whereas the two planes A/C and B/D separate two moieties that are no longer mirror images (the *DD*-configuration of a chain should correspond the *LL*-configuration of the opposite chain). Therefore, C-1 and C-3 carbons, for instance, are no longer equivalent and give two distinct signals. However, a *C*<sub>4</sub> symmetry axis is still present, since the chains, including the chiral center, are superimposable after a 90° rotation. The C-1 carbon will thus be equivalent to C-7, C-13, and C-19 and C-3 will coincide with C-9, C-15, and C-21. Carbons (and protons) equidistant from the chiral centers, such as C-*e*/C-*i* (or H-*e*/H-*i*), show a single signal as also observed in the achiral resorc[4]arene **1** precursor, whereas all of the other nuclei cumulatively produce two signals. The distribution pattern of carbons and protons in Tables 1S–3S (Supporting Information) is in agreement with these considerations.

**Physical Characterization of *N*-Linked Peptidioresorc[4]arenes.** Physical properties of *N*-linked peptidioresorc[4]arenes are summarized in Table 1. In the ESI-HRMS characterization of peptidioresorc[4]arene benzyl esters **10**, **11**, and **16** (positive mode), a strong tendency was observed to form complexes with sodium (Na) and potassium (K) ion impurities, as already reported.<sup>10a</sup> The most intense peak in the spectrum was that for the double charged sodium adduct ion  $[M + 2Na]^{2+}$ , at *m/z* 1043.53604–1043.53656 for **10** and **11** (which are indeed regioisomers), and at *m/z* 1228.01773 for **16**. The corresponding monocharged species,  $[M + Na]^+$ , were also observed. The free acids **12** and **13**, which are indeed regioisomers, displayed in the mass spectra (negative mode) the most abundant ion corresponding

to the fully deprotonated molecule as sodium adduct ( $[M - 4H + Na]^{3-}$ ), at *m/z* 566.61975–566.62079, in agreement with their molecular formula. For free dicarboxylic acids **17a,b**, a diagnostic peak at  $[M - 2H]^{2-}$  was found in the mass spectrum (negative mode), at *m/z* 843.32839–843.33097. Melting points were normally restricted in a 1.0 °C interval, but the free dicarboxylic acids (–)-**17a** and (+)-**17b** decomposed instead of melting. Finally, optical rotations for the two members of each enantiomeric pair were comparable in most cases (see Table 1), excluding any significant racemization. However, for the enantiomeric pairs **12a,b** and **13a,b** quite different values were obtained (vide infra). Notably, the signs of optical rotation are correlated with the stereochemistry of peptidioresorc[4]arenes: the *L,L*-series always show negative values.

**Circular Dichroism (CD) and Enantioselective HPLC Analysis.** The discrepancy between the optical rotations of the *DD*- and *LL*-forms of compounds **12** and **13** prompted us to examine their enantiomeric purity by circular dichroism (CD) measurements and enantioselective HPLC analysis.

The UV spectra in TRIS buffer 0.1 M at pH 7.4 of both **12** and **13** couples of enantiomers (Figure 4a,b, top traces) exhibit absorption bands at the same wavelength maxima (210 and 280 nm) attributed to the expected <sup>1</sup>*L*<sub>a</sub> and <sup>1</sup>*L*<sub>b</sub> electronic transitions.<sup>14</sup> On the contrary, the CD spectra of each enantiomeric (–)-**12a**/(+)-**12b** and (–)-**13a**/(+)-**13b** pair are mirror images (Figure 4a,b, bottom traces) and display the bisignate Cotton effect centered at the above-mentioned wavelengths.

The first approach by enantioselective HPLC with a teicoplanin-based column (CHIROBIOTIC T)<sup>15a</sup> led to the enantioselective discrimination of the **12a/12b** pair, but not **13a/13b**. By contrast, the enantiomeric pairs of both free acids were successfully separated using a CHIRALPAK QN-AX (8S,9R) column, which has been proved to perform highly enantioselective separations of a very broad spectrum of chiral acids, such as *N*-derivatized amino acids, α-aryloxyalkyl and α-arylalkyl carboxylic acids like profens.<sup>15b–d</sup> In fact, such a column, based on a quinine (QN)-carbamate derivative (Figure 1S, Supporting Information), is a weak anionic exchanger and is able to perform electrostatic interactions between oppositely charged functionalities of the analyte and the chiral selector bonded. Enantiomeric excesses (ee, %) of peptidioresorc[4]arenes **12a,b** and **13a,b**, checked by enantioselective HPLC on the above-mentioned column, were in the 95–97% range.

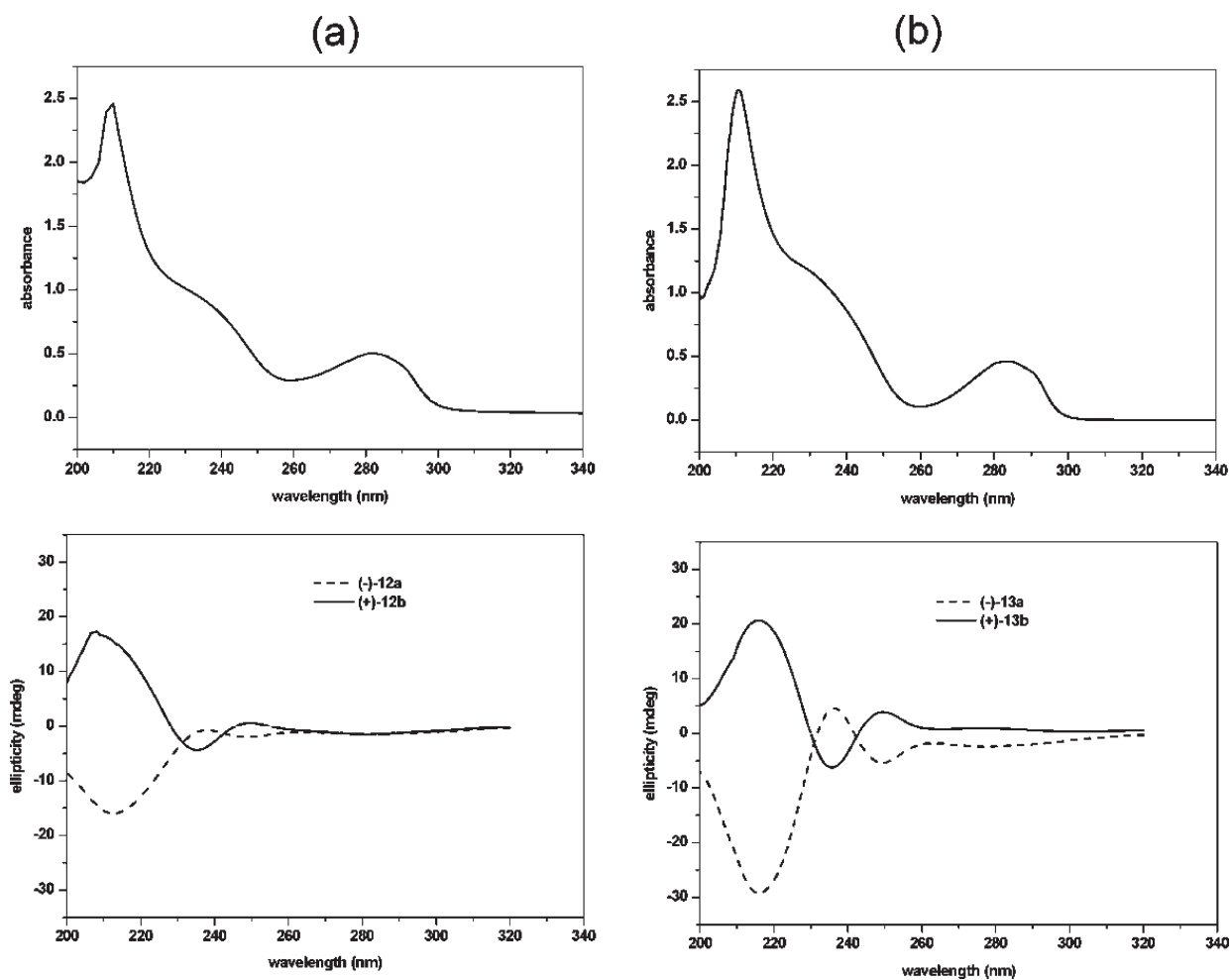


Figure 4. UV (top traces) and CD (bottom traces) spectra in TRIS buffer 0.1 M at pH 7.4 of enantiomeric resorc[4]arenes (a) (–)-12a/(+)-12b and (b) (–)-13a/(+)-13b ( $4.0 \times 10^{-5}$  M).

**Preliminary Binding Studies with HSA.** The ability of *N*-linked peptidoresorc[4]arenes to establish interactions with proteins was preliminary tested on HSA. To demonstrate the effective binding of receptor **12** to HSA, a CD experiment was carried out with a double sector quartz cuvette. Solutions of HSA ( $5 \times 10^{-6}$  M) and of resorcarene derivatives (–)-12a or (+)-12b ( $5 \times 10^{-6}$  M) in 0.005 M sodium phosphate buffer (pH = 7.4) were introduced separately into each sector of the cuvette. A series of CD spectra were recorded before mixing the two solutions (Figure 5, top traces a,b, solid lines) and a second one after mixing (dotted lines). The CD spectra before mixing showed intense negative bands at ~208 and 222 nm, which are typical of proteins with high  $\alpha$ -helical content. The corresponding spectra obtained after the mixing with receptors (–)-12a and (+)-12b were similar in shape, indicating that the structure of HSA after mixing is still predominantly  $\alpha$ -helical. The difference between the spectra of resorcarene derivatives collected after and before the mixing with HSA provided CD spectra (Figure 5, bottom traces a,b, dotted lines), which, as compared with the respectively normalized spectra (solid lines), showed a consistent change in the absorptions. The differences between the spectral profiles and peak positions of the resorcarene CD bands before and after mixing with HSA indicate that the molecule is located in a dissymmetric environment after exposure to the protein. These observations indicate

the formation of a complex between HSA and the resorcarene derivative, not affecting the structural integrity of HSA.

**Initial Screening for Inhibition Activity.** The inhibition activity of the synthesized *N*-linked peptidoresorc[4]arenes was evaluated by *in vitro* assays with a chromogenic substrate toward bovine pancreatic  $\alpha$ -chymotrypsin ( $\alpha$ -ChT), a serine protease which was already shown to be inhibited by a specific family of calix[4]arene receptors.<sup>9b</sup> ChT hydrolyzes proteins selectively attacking the protein chain next to aromatic residues such as tyrosine (Tyr) and phenylalanine (Phe), but it has also affinity for other amino acids bearing apolar side chains (e.g., methionine, leucine).<sup>16</sup> The protein, which is characterized by the presence of positive charges on its surface, as suggested by the isoelectric point of 8.8, has been considered a suitable target for studying the interaction with receptors containing terminal carboxylic acids, in anionic form at the physiological pH.<sup>7,12</sup> At the same pH, some basic amino acids surrounding the active site are protonated: electrostatic interactions with the positively charged patches of ChT are thus expected to lead to a consequent inhibition of the enzyme. Inhibition assays should thus provide a useful handle for studying the protein–receptor complex.

Inhibition of ChT by peptidoresorc[4]arenes free acids **12** and **13** was investigated by monitoring at 405 nm the rate of

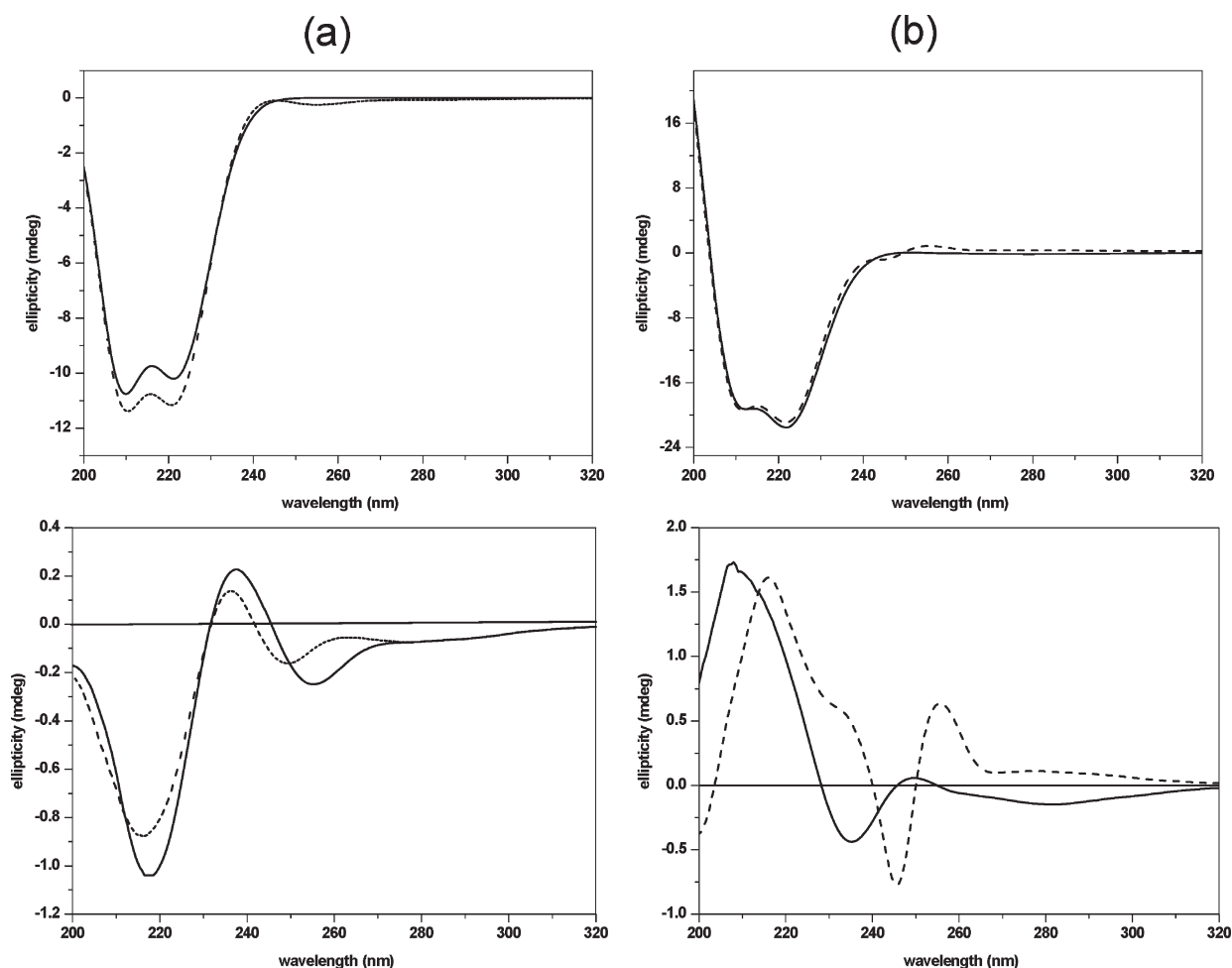


**Figure 5.** Top traces: CD spectra obtained in a double sector cuvette of HSA ( $5 \times 10^{-6}$  M) in 0.005 M sodium phosphate buffer (pH = 7.4) before (solid lines) and after (dotted lines) mixing with (a) (–)-**12a** ( $5 \times 10^{-6}$  M) or (b) (+)-**12b** ( $5 \times 10^{-6}$  M) solutions. Bottom traces: CD spectra of (a) (–)-**12a** or (b) (+)-**12b** obtained by the difference between the spectra after and before the mixing with HSA (dotted lines), compared with the respectively normalized spectra (solid lines).

enzymatic hydrolysis of the chromogenic substrate *N*-succinyl-Ala-Ala-Pro-Phe-*p*-nitroanilide (Suc-AAPF-*p*NA) to *p*-nitroaniline, after the mixing of protein and receptors. Control experiments were carried out under identical conditions without the addition of resorc[4]arenes. The inhibitory effect, determined by treating the enzyme ( $4.0 \times 10^{-8}$  M) with solutions of **12a**, **12b**, **13a**, or **13b** ( $4.0 \times 10^{-5}$  M) in 0.005 M sodium phosphate buffer for various preincubation periods followed by addition of Suc-AAPF-*p*NA in 2-methoxyethanol (cosolvent), was shown to be time-independent (see Table 2). Receptors (–)-**12a** and (+)-**12b** were found to decrease the Suc-AAPF-*p*NA hydrolysis to 13 and 11%, respectively, as compared with those of the untreated enzyme, whereas (–)-**13a** and (+)-**13b** led to a smaller inhibition. The major inhibition by the pair **12a/12b** (with the valyl-leucine instead of leucyl-valine sequence) can be attributed to a preference of the enzyme for the cleavage of dipeptide chains containing leucine next to hydrophobic residues. The dipeptide configuration seems to be not so important, even though the *DD*-derivatives were slightly more active than the *LL*-enantiomers, which are the natural ligands of the enzyme.

**Peptidoresorc[4]arene (+)-12b.** To get more information on the inhibition mechanism of peptidoresorc[4]arenes toward ChT, we focused our attention on the most effective inhibitor

(+)-**12b**, which was treated at concentrations ranging from  $4.0 \times 10^{-6}$  to  $1.0 \times 10^{-4}$  M with ChT maintained at a fixed concentration ( $4.0 \times 10^{-8}$  M) for a 90 min preincubation period. The dose-responsive inhibition of ChT by (+)-**12b** at pH 7.4 in 0.005 M sodium phosphate buffer showed that, in the presence of (+)-**12b** at a  $4.0 \times 10^{-6}$  M concentration, the activity of ChT decreased to 43% (this value represents an average of three independent sets of experiments, SD < 3%). Further increase in the concentration of (+)-**12b** ( $4.0 \times 10^{-5}$  M) resulted in a decrease of the initial velocity to 11% (dose-responsive inhibition plots are reported in Figure 2S, Supporting Information). Nonlinear regression analysis to fit the Michaelis–Menten data (Figure 6, top) yielded the apparent maximum enzymatic reaction rate ( $V_{\max} = 7.3 \times 10^{-3}$  abs sec $^{-1}$ ) and the Michaelis–Menten constant ( $K_m = 96.9 \pm 7.2$   $\mu$ M), whereas Dixon plots<sup>17a</sup> (Figure 6, bottom right) were used to measure the inhibition constant ( $K_i = 12.4 \pm 5.1$   $\mu$ M). The kinetic studies pointed out that receptor (+)-**12b** behaves as a noncompetitive inhibitor of ChT because it decreases the  $V_{\max}$  values, with minor effects on the  $K_m$  constant.<sup>17b</sup> On these bases, it can be envisaged that (+)-**12b** does not compete directly with the substrate molecules, though it may affect the size and shape of the catalytic cleft.

**Table 2.** Residual Activity (%) of ChT ( $4.0 \times 10^{-8}$  M) after Mixing with Peptidoresorc[4]arenes **12**, **13**, **16**, and **17** in Comparison with the Activity of the Native Enzyme

Compd	Configuration	Receptor concentration	Residual activity (%)	Dependence on time of inhibition activity
(-)- <b>12a</b>	(L,L)	$4.0 \times 10^{-5}$ M	13	Time-independent
(+) - <b>12b</b>	(D,D)	$4.0 \times 10^{-6}$ M	43	Time-independent
	(D,D)	$4.0 \times 10^{-5}$ M	11	
	(D,D)	$1.0 \times 10^{-4}$ M	0	
(-)- <b>13a</b>	(L,L)	$4.0 \times 10^{-5}$ M	25	Time-independent
(+) - <b>13b</b>	(D,D)	$4.0 \times 10^{-5}$ M	17	Time-independent
(-)- <b>17a</b>	(L,L)	$4.0 \times 10^{-6}$ M	28	Time-independent
	(L,L)	$4.0 \times 10^{-5}$ M	5	
(+) - <b>17b</b>	(D,D)	$4.0 \times 10^{-5}$ M	71 → 100	Decreases by the time
(+) - <b>10b</b>	(D,D)	$4.0 \times 10^{-6}$ M	68	Time-independent
	(D,D)	$4.0 \times 10^{-5}$ M	5	
(-)- <b>16a</b>	(L,L)	$4.0 \times 10^{-7}$ M	60	Time-independent
	(L,L)	$4.0 \times 10^{-6}$ M	5	
(+) - <b>16b</b>	(D,D)	$4.0 \times 10^{-6}$ M	13 → 6	Increases by the time

To determine some possible binding areas of (+)-**12b** on the surface of ChT, a computational docking experiment was carried out using the program AutoDock 4.0.<sup>18</sup> The calculations point to a complex of the type shown in Figure 7, where the carboxylate groups in (+)-**12b** make electrostatic interactions with several of the basic residues (Lys-36, Lys-90, Lys-175, and Arg-145) surrounding the active site cleft of ChT. Some of these amino acids were already found to be involved in ChT complexes with calix-[4]arene receptors.<sup>9b,d</sup>

The proposed ChT inhibition by peptidoresorc[4]arene (+)-**12b** through a specific complex formation was confirmed by nondenaturing gel electrophoresis on 1% agarose gel at pH 7.4 (Figure 8).<sup>9b,g</sup> In the absence of receptor (lane 1), the protein (ChT,  $2.0 \times 10^{-5}$  M) migrated almost completely toward the cathode, in agree with its positively charged surface. At a (+)-**12b**/ChT molar ratio of 1:1 (lane 2), two bands were observed and attributed to unbound ChT (near to the cathode) and to a complex between ChT and (+)-**12b**, which migrated toward the anode. When the concentration of receptor (+)-**12b** was increased to  $1.0 \times 10^{-4}$  M (lane 3) and to  $2.0 \times 10^{-4}$  M (lane 4), the majority of ChT molecules appeared to be bound to receptor (+)-**12b**, as shown by the lower intensity of the bands in the cathode region. At a (+)-**12b**/ChT molar ratio of 50:1 (lane 5), only the band corresponding to the bound ChT was observed. To sum up, comparison of the lanes shows that ChT and receptor (+)-**12b** form a new species with different polarity to uncomplexed enzyme. Since no free enzyme appeared on the gel starting from lane 4, the binding ratio of (+)-**12b**/ChT should be between 10:1 and 50:1.

The change in mobility of ChT after addition of receptor (+)-**12b** may depend on both an increased size and an attenuation of the enzyme surface charge due to binding and complex formation: several cationic residues are indeed present near the active site cleft of ChT. These findings suggested that complexation between ChT and (+)-**12b** resulted in the formation of neutral particles but gave no information on the type of binding, which was assumed to be primarily, but not purely, electrostatic.

To shed light on some other possible interactions between peptidoresorc[4]arenes and ChT, the investigation was extended to the available benzyl ester (+)-**10b**, which was the synthetic precursor of the analyzed free acid. The inhibition experiments, carried out under the same conditions as for (+)-**12b** (see Table 2), resulted in only 5% residual activity of the enzyme after incubation with (+)-**10b** at a concentration of  $4.0 \times 10^{-5}$  M, increasing to 68% with the macrocycle at  $4.0 \times 10^{-6}$  M (time-independent inhibition). A different type of interaction, actually hydrophobic, by peptidoresorc[4]arenes was thus shown to be possible for the ChT inhibition (vide infra), since free acid (+)-**12b** was a much weaker inhibitor of ChT than its benzyl ester homochiral precursor (+)-**10b**.

**Peptidoresorc[4]arenes 17a,b.** The receptors pair **17a/17b** features a change in the nature of the dipeptide chain (valyl-aspartic acid instead of valyl-leucine, as compared with **12a/12b**), but mainly a 2-fold number of ionizable carboxylic groups and, as expected, a major amount of electrostatic interactions. However, only the LL-derivative (-)-**17a** exhibited a larger inhibition activity than the homochiral (-)-**12a** (see Table 2) at the same concentration: numerically, only 5% of residual activity of ChT was found at a concentration of  $4.0 \times 10^{-5}$  M. The inhibition resulted to be time-independent and was still significant (28% of residual ChT activity) at a  $4 \times 10^{-6}$  M concentration of receptor. Surprisingly, in the presence of the DD-derivative (+)-**17b**, ChT exhibited a 71% of residual activity after 90 min. The inhibitory activity of (+)-**17b** was shown to be time-dependent (100% of residual ChT activity was found after 180 min). As in the case of (+)-**12b**, for comparative purposes we tested the inhibition activity of benzyl esters (-)-**16a** and (+)-**16b**, which were the synthetic precursors of receptors **17a,b**: in these cases, because the benzyl esters were slightly soluble in phosphate buffer, higher concentrations than  $4 \times 10^{-6}$  M were not allowed, and the cosolvent (2-methoxyethanol) was replaced by dimethyl sulfoxide (DMSO) for the preparation of stock solutions of receptors. The final concentration of DMSO ( $2.4 \times 10^{-2}$  M) was indeed much lower than those needed for influencing

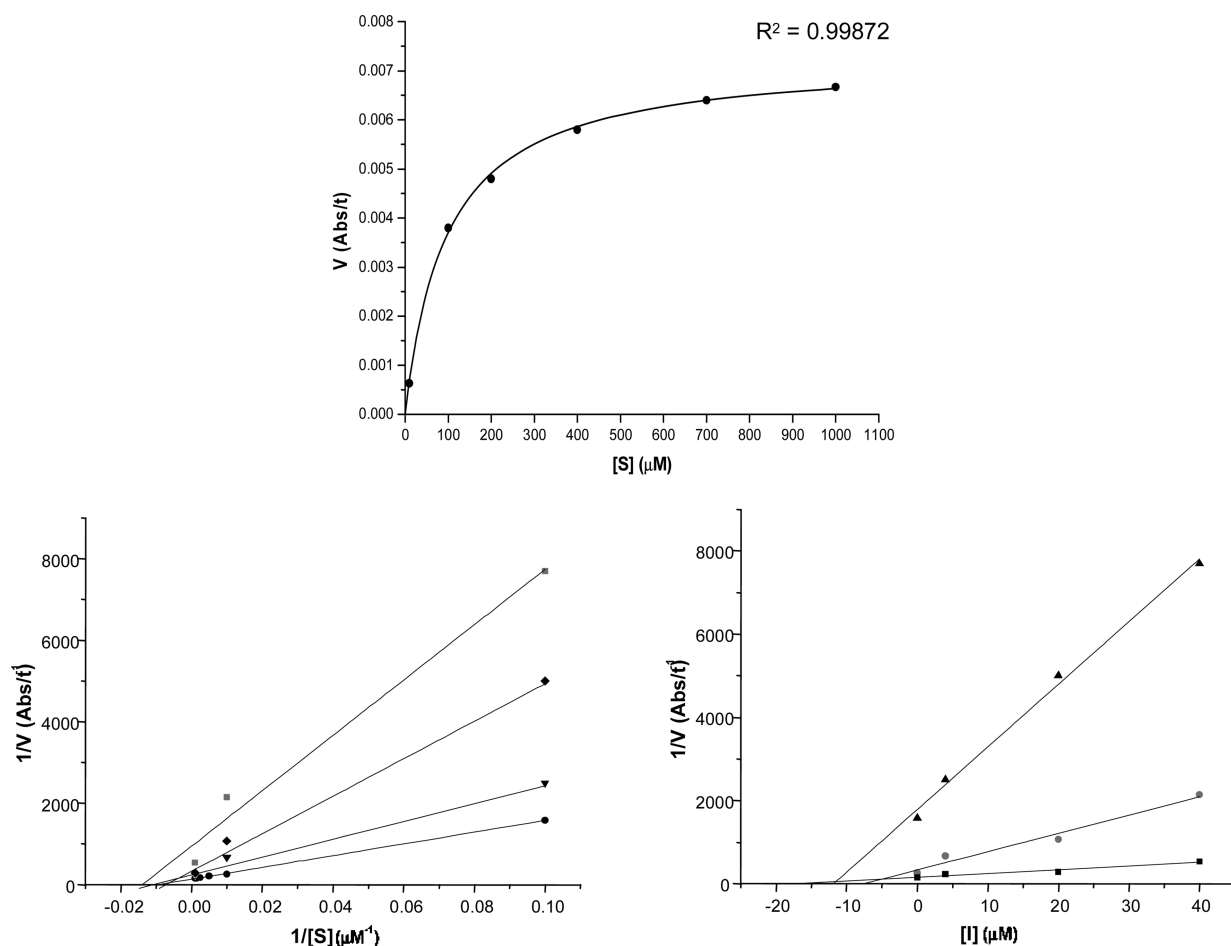


**Figure 6.** Noncompetitive inhibition of ChT ( $4.0 \times 10^{-8}$  M) by receptor (+)-12b. Top: nonlinear regression analysis to fit the Michaelis–Menten data in the absence of inhibitor ( $K_m = 96.9 \pm 7.2 \mu\text{M}$ ). Left: Lineweaver–Burk plot at three fixed Suc-AAPF-*p*NA concentrations in the absence (●) and presence of  $4 \mu\text{M}$  (▼),  $20 \mu\text{M}$  (◆), and  $40 \mu\text{M}$  (■) of (+)-12b. Right: Dixon plot at three fixed Suc-AAPF-*p*NA concentrations, namely (▲) 10, (●) 100, and (■)  $1000 \mu\text{M}$ .  $K_i = 12.4 \pm 5.1 \mu\text{M}$ .

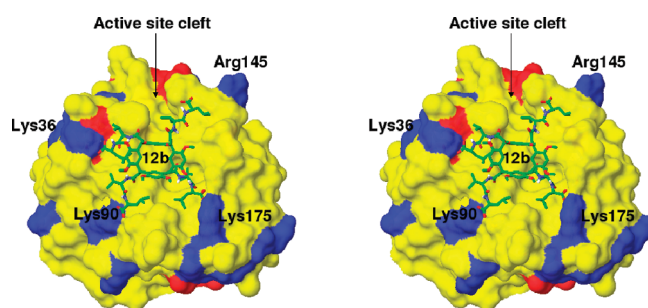


**Figure 7.** Calculated structure (crossed stereoview by AutoDock 4.0) for the interaction of (+)-12b with ChT. The protein structure is displayed as a Connolly surface, while the 3D structure of the docked ligand is explicitly shown colored by atom type. Uncharged amino acids are colored in yellow, negatively charged in red and positively charged in blue. Few relevant basic residues are tagged. The active site cleft entrance is marked by a black arrow.

the enzyme activity.<sup>19</sup> In the presence of receptor (+)-16b, the residual activity of ChT decreased by the time to 13% after 90 min to reach a minimum (6%) after 120 min. The time-dependent inhibition supports the slow formation of a network

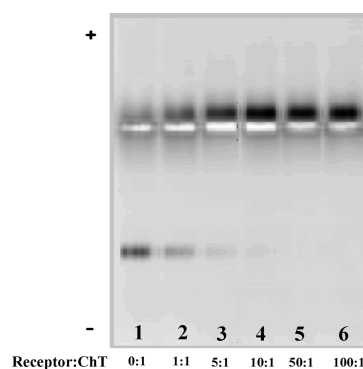


**Figure 8.** Nondenaturing gel electrophoresis of ChT and receptor (+)-12b on 1% agarose gel at pH 6.0. Samples were loaded in the middle of the gel: lane 1, ChT ( $2.0 \times 10^{-5}$  M); lanes 2–5, (+)-12b + ChT at increasing receptor-to-ChT molar ratios; lane 6, (+)-12b ( $2.0 \times 10^{-5}$  M).

of weak hydrophobic interactions. Moreover, the LL-enantiomer (–)-16a was shown to be the most potent inhibitor of ChT of all the family of peptidoresorc[4]arenes: 5% of residual activity of the enzyme was found in the presence of (–)-16a at a concentration

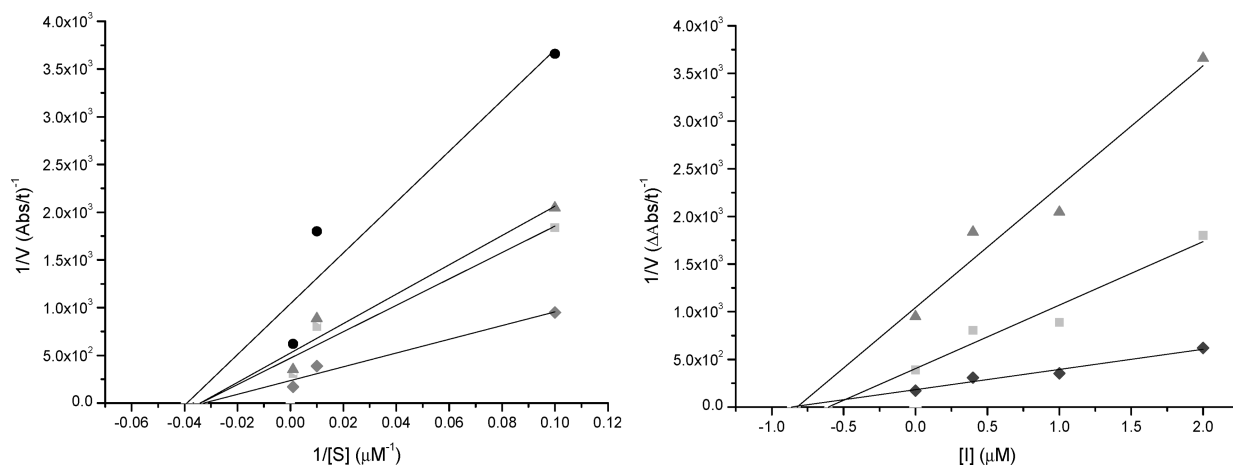


**Figure 9.** Noncompetitive inhibition of ChT ( $4.0 \times 10^{-8}$  M) by receptor (–)-16a. Left: Lineweaver–Burk plot at three fixed Suc-AAPF-pNA concentrations in the absence (◆) and presence of 0.4  $\mu\text{M}$  (■), 1  $\mu\text{M}$  (▲), and 2  $\mu\text{M}$  (●) of (–)-16a. Right: Dixon plot at three fixed Suc-AAPF-pNA concentrations, (▲) 10  $\mu\text{M}$ , (■) 100  $\mu\text{M}$ , and (◆) 1000  $\mu\text{M}$ .  $K_i = 0.76 \pm 0.14$   $\mu\text{M}$ .

of  $4.0 \times 10^{-6}$  M, and 60% at  $4.0 \times 10^{-7}$  M (dose-responsive inhibition plots of ChT by (–)-16a are reported in Figure 3S, Supporting Information). Notably, the inhibition was immediate and time-independent. The fact that LL-conformation of dipeptides is coincident with the stereochemistry of the natural substrates of the enzyme is not enough to explain the unexpected results for interactions based exclusively on hydrophobicity.

**Peptidoresorc[4]arene (–)-16a.** To get more information on the unexpected strong inhibition of benzyl ester (–)-16a toward ChT, we performed the same set of experiments as for free acid (+)-12b (vide supra). Receptor (–)-16a was thus treated at concentrations ranging from  $4.0 \times 10^{-7}$  to  $4.0 \times 10^{-6}$  M with ChT maintained at a fixed concentration ( $4.0 \times 10^{-8}$  M) for a 90 min preincubation period. Kinetic analysis, based on Lineweaver–Burk (Figure 9, left) and Dixon (Figure 9, right) plots, pointed out that receptor (–)-16a is a noncompetitive inhibitor of ChT ( $K_i = 0.76 \pm 0.14$   $\mu\text{M}$ ) because it decreases the  $V_{\text{max}}$  values without affecting the  $K_m$  constant.<sup>17</sup> However, receptor (+)-12b, featuring more complementary recognition surfaces to ChT than receptor (–)-16a, showed a significantly lower inhibition potency ( $K_i = 12.4 \pm 5.1$   $\mu\text{M}$ ). To explain such strong interaction between benzyl ester (–)-16a and ChT we may invoke the chemical similarity between the terminal benzyl groups and the benzyl side chain of Phe; in fact, examination of the specificity requirements for ChT reveals that a critical interaction for efficient binding of a substrate to this enzyme includes a van der Waals interaction of the benzyl side chain of Phe with a hydrophobic pocket adjacent to the active site of the enzyme.<sup>7a</sup>

**Effect of Medium Ionic Strength on the Protein–Receptor Complexation.** The noncovalent binding experiment performed by nondenaturing gel electrophoresis (Figure 8, lanes 2–5) showed that the binding process between inhibitor (+)-12b and ChT must be reversible. Therefore, we investigated the possible occurrence, for the bound enzyme, to be released from the macrocycle surface when the ionic strength of the medium is increased. ChT ( $4.0 \times 10^{-8}$  M) was thus incubated with inhibitor (+)-12b ( $4.0 \times 10^{-5}$  M) in the presence of sodium chloride (NaCl) at five different concentrations ranging from  $1.0 \times 10^{-4}$  to  $1.0 \times 10^{-1}$  M, as already reported.<sup>6e,7b</sup> The samples were incubated at room temperature for 90 min, a time sufficient for an almost complete inhibition ( $\sim 90\%$ ) in the absence of NaCl. The

enzyme activity was monitored as above-described and compared with the activity of a control solution containing only ChT and NaCl under the same conditions (system named before mixing, BM). The normalized residual activities of each sample and the corresponding NaCl concentration are summarized in Table 3.

In a second system (named after mixing, AM), NaCl at the above-mentioned concentrations was added to the complex ChT/(+)-12b, as well as to a solution of pure ChT, after 90 min incubation period. Both mixtures were analyzed after further 90 min of incubation. This method was used to evaluate the effect of ionic strength on the stability of the complex ChT/(+)-12b, once allowed to form; the results, i.e., the residual activities of the enzyme and the corresponding NaCl concentrations, are also collected in Table 3.

As expected, the residual activity of ChT increases with the increase of NaCl concentration (BM mode): at NaCl concentrations between  $1.0 \times 10^{-4}$  and  $1.0 \times 10^{-2}$  M (see Table 3), the ionic strength is not strong enough to break completely the electrostatic attraction between enzyme and inhibitor, and the residual activity undergoes a small increase (23% and 36% of the control). By contrast, the ChT residual activity increases sharply in the presence of  $5.0 \times 10^{-2}$  M NaCl (95% of the control) and is almost completely restored ( $\sim 98\%$ ) for NaCl  $1.0 \times 10^{-1}$  M. These findings confirm that the binding of inhibitor (+)-12b to the enzyme is mostly based on electrostatic complementarities and, as such, is reversible and does not denature the native conformation of ChT.

When we performed the same set of experiments on receptor (–)-17a, which features a 2-fold number of ionizable carboxylic groups for the replacement of leucine with an aspartate residue, we observed that the formation of the complex ChT-receptor seemed to be mitigated only partially by the increase of the ionic strength: actually, the residual activity of the enzyme is still 50% in the presence of NaCl  $1.0 \times 10^{-1}$  M (Table 3, system BM). This result may be attributed to the higher number of ionizable functional groups, and thus to a major amount of electrostatic interactions to be broken.

The AM mode experiments, aimed at investigating the stability of the complex ChT-receptor under the influence of the medium ionic strength, substantially confirmed the mainly electrostatic



**Table 3. Residual Activity (%) of ChT ( $4.0 \times 10^{-8}$  M) in the Presence of NaCl before Mixing (System BM) and after Mixing (System AM) with Peptidoresorc[4]arenes (+)-12b, (-)-17a, (+)-10b, (+)-16b, and (-)-16a, in Comparison with the Activity of the Native Enzyme**

compd <sup>a</sup>	system	NaCl					
		0 M	$1.0 \times 10^{-4}$ M	$1.0 \times 10^{-3}$ M	$1.0 \times 10^{-2}$ M	$5.0 \times 10^{-2}$ M	$1.0 \times 10^{-1}$ M
(+)-12b	BM	11	23	36	36	95	98
	AM	8	10	10	20	62	92
(-)-17a	BM	5	3	5	5	17	50
	AM	3	4	3	10	64	100
(+)-10b	BM	5				9	51
	AM	6				11	15
(+)-16b	BM	13	13	13	12	17	32
	AM	13	16	13	14	22	40
(-)-16a	BM	4	5	4	3	2	2
	AM	1	1	1	2	2	2

<sup>a</sup> Receptors concentration:  $4.0 \times 10^{-5}$  M, except for receptors (-)-16a and (+)-16b ( $4.0 \times 10^{-6}$  M).

nature of the interaction between ChT and receptors (+)-12b and (-)-17a (the first complex is slightly more stable). Also in this case, the investigation on (+)-12b was extended to the available benzyl ester (+)-10b, which was its synthetic precursor: the enzyme restored only partially its activity, which was 51% in the presence of NaCl  $1.0 \times 10^{-1}$  M (Table 3, system BM), denoting a low importance of ionic strength on the quality of interaction between ChT and benzyl ester (+)-10b. As a confirmation, the stability of the complex was shown to be slightly influenced by the ionic strength as well, since, at the same NaCl concentration, ChT showed only 15% residual activity (AM mode).

With regard to receptor (+)-16b, which was supposed to slowly form a network of hydrophobic interactions with ChT (see Table 2), the experiments in the presence of increasing concentrations of NaCl confirmed such hypothesis (see Table 3). In fact, the reduced influence of the ionic strength on the formation (system BM) and the stability (system AM) of the ChT-(+)-16b complex is evidenced by the values of 32% and 40%, respectively, recovered at NaCl  $1.0 \times 10^{-1}$  M for the residual ChT activity. Notably, the LL-enantiomer (-)-16a was confirmed to be the most effective inhibitor of ChT activity, since the inhibition was not significantly affected by the ionic strength (Table 3), both before and after incubation of the inhibitor with enzyme.

## CONCLUSIONS

Our efforts into the design of novel N-linked peptidoresorc[4]arenes with appropriately modified functional groups proved that they are able to interact with proteins such as HSA and acquire inhibition properties vs enzymes such as ChT. For compounds with terminal carboxylate functions (12, 13, and 17), the ChT inhibition is based essentially on electrostatic interaction, and the bound enzyme can be released from the resorcarene surface by increasing the ionic strength, with its activity almost completely restored. The inhibitors were not modified by ChT, as checked by TLC analysis ( $\text{CHCl}_3/\text{MeOH}$  mixtures) of mixtures of peptidoresorc[4]arenes and enzyme incubated for 3 h, after complex denaturation. For receptors with terminal benzyl ester groups (10 and 16) a hydrophobic network can be instead suggested. A computational docking experiment carried out on (+)-12b pointed to a complex where the carboxylate groups make electrostatic interactions with several of the basic residues

(Lys-36, Lys-90, Lys-175, and Arg-145) surrounding the active site cleft of ChT. Within the same framework, the benzyl ester derivatives seem to be more effective: for example, free acid (+)-12b is a much weaker inhibitor of ChT than its benzyl ester homochiral precursor (+)-10b, as judged by the residual enzymatic activity after a 90 min incubation period. In the cases of receptors 12 and 13, compounds with D,D-configuration were more active than the L,L-derivatives. In particular, receptor (+)-12b was shown to be a noncompetitive inhibitor of ChT ( $K_i = 12.4 \pm 5.1 \mu\text{M}$ ) because it decreases the  $V_{\text{max}}$  values without affecting the  $K_m$ . However, for all of the other cases, the most active compounds featured the L,L-configuration, which is the sterical arrangement of the natural ligand. This is mainly true for the 17a/17b pair: the arrangement of the eight carboxylate groups, responsible for electrostatic interaction with the enzyme seems to be significantly affected by the D,D-configuration of the dipeptide chains (71% of residual enzymatic activity vs 5%). This trend was observed on the benzyl ester homochiral precursor as well, where the LL-enantiomer (-)-16a was found to be the most effective noncompetitive inhibitor of ChT activity, with a  $K_i = 0.76 \pm 0.14 \mu\text{M}$ . In this case, inhibition was not significantly affected by the ionic strength, both before and after mixing of the inhibitor with enzyme.

Focusing on the nature of the dipeptide chains, we noticed that the terminal amino acids of peptidoresorc[4]arenes 12, 13 and 17 could be placed in the following scale of inhibition activity: aspartic acid (receptor 17) > leucine (receptor 12) > valine (receptor 13), somehow corresponding to the 2-fold number of interaction sites (for aspartic acid) and to the affinity of ChT for the amino acids (for leucine), as a substrate.<sup>16</sup> Analogously, to explain the strong hydrophobic interactions between ChT and peptidoresorc[4]arenes benzyl esters 10 or 16, we may invoke the chemical similarity between the terminal benzyl groups and the benzyl side chain of phenylalanine, one of the main substrates of ChT.<sup>16</sup> In fact, a van der Waals interaction of the Phe benzyl side chain with a hydrophobic pocket adjacent to the active site is one of the specificity requirements for ChT.

## EXPERIMENTAL SECTION

**Materials.**  $\alpha$ -Chymotrypsin (Type II) from bovine pancreas (ChT), N-succinyl-Ala-Ala-Pro-Phe-p-nitroanilide (Suc-AAPP-pNA),

HPLC-grade acetonitrile, water, and glacial acetic acid were purchased from Sigma Aldrich. HPLC-grade ammonium acetate was purchased from Baker. Dimethyl sulfoxide (DMSO) and 2-methoxyethanol (analytical grade) were from Carlo Erba. Reagents for electrophoresis were purchased from commercial sources.

**Synthesis of Resorc[4]arene Octamethyl Ethers 1–3.** Compounds 1–3 were synthesized as previously described.<sup>10a</sup>

**Preparation of *N*-Boc-D-aspartic Acid.** To an ice-cooled solution of D-aspartic acid in 1,4-dioxane (1.5 g, 11.3 mmol in 20 mL) were added NaOH 1 N (45 mL) and di-*tert*-butyl dicarbonate (2.5 g, 11.5 mmol). The mixture was left at room temperature for 3 h, acidified to pH 1–2 with HCl 1 N, and extracted with ethyl acetate (5 × 80 mL). The pooled organic extract, after drying over Na<sub>2</sub>SO<sub>4</sub>, gave *N*-Boc-D-aspartic acid with a 63% yield.

**General Procedure for the Preparation of Benzyl Esters 5b, 8b, and 14b as TFA Salts.** Cs<sub>2</sub>CO<sub>3</sub> (32.6 g, 100 mmol) was added to an ice-cooled solution of the proper *N*-Boc-protected D-amino acid (100 mmol) in DMF (200 mL). The mixture was stirred at 0 °C for 45–60 min. Benzyl bromide (11.9 mL, 17.1 g, 100 mmol) was added to the reaction mixture, which was maintained under magnetic stirring at 0 °C for 30 min and allowed to reach room temperature overnight. The reaction mixture was poured into H<sub>2</sub>O (800 mL) and extracted with *n*-hexane (4 × 250 mL). The combined extracts were washed with H<sub>2</sub>O (200 mL) and saturated NaCl, and then dried over Na<sub>2</sub>SO<sub>4</sub>. Filtration, concentration, and drying under vacuum gave *N*-Boc-D-leucine benzyl ester (95%) *N*-Boc-D-valine benzyl ester (95%) and *N*-Boc-D-aspartic acid dibenzyl ester (86%) as colorless oils. Benzyl esters (1 mmol) were deprotected by treatment with TFA–DCM (1:1, 25 mL). The reaction mixture was stirred at 25 °C for 45 min and then evaporated to dryness; the addition of a suitable hexane/Et<sub>2</sub>O mixture (50 mL) under vigorous stirring yielded white solids that were filtered, washed several times with hexane/Et<sub>2</sub>O, and dried under vacuum to afford the pure TFA salts 5b, 8b, and 14b in quantitative yields. For the characterization of the above compounds, see the Supporting Information.

**General Procedure for the Preparation of Dipeptide Benzyl Esters 6a,b, 9a,b, and 15a,b as TFA Salts.** The proper amino acid benzyl ester as TFA or *p*-toluenesulfonate salt (5.5 mmol), HOBT (0.75 g, 5.5 mmol), Et<sub>3</sub>N (0.96 mL, 7.1 mmol), and the proper *N*-Boc-protected amino acid (5.5 mmol) were dissolved in DCM (250 mL). DCC (1.14 g, 5.5 mmol) was added to the solution cooled in an ice bath. After 4 h at room temperature, the solvent was removed under vacuum, and the residue was purified by silica gel column chromatography (hexane–ethyl acetate, 7.5:2.5) to yield the *N*-Boc-protected dipeptide benzyl esters as white powders (yields 80–85%). Dipeptides (0.9 mmol) were deprotected by treatment with TFA–DCM (1:1, 25 mL) as described previously to afford the pure TFA salts 6a,b, 9a,b, and 15a,b in quantitative yields. For the characterization of the above compounds, see the Supporting Information.

**2,8,14,20-Tetrakis(L-valyl-L-leucinamido)resorc[4]arene Benzyl Ester (10a).** DIPEA (0.42 mL, 2.5 mmol) was added under nitrogen to a dry THF solution of tetracarboxylic acid chloride 3 (150 mg, 0.15 mmol in 45 mL). The mixture was stirred for 40 min at room temperature, and a dry THF solution of 6a (322 mg, 0.9 mmol in 30 mL) was added dropwise in a 1 h period. The reaction mixture was held at reflux under nitrogen for 1 h. Evaporation of the solvent and purification by column chromatography (CHCl<sub>3</sub>/MeOH mixtures) gave peptido-resorc[4]arene (–)-10a as a pale yellow powder (70% overall yield). Mp: 220–221 °C. <sup>1</sup>H and <sup>13</sup>C NMR signals are reported in the Supporting Information (Tables 1S and 2S). ESI-HRMS (pos): *m/z* found 1043.53604 ([M + 2Na]<sup>2+</sup>), C<sub>116</sub>H<sub>152</sub>O<sub>24</sub>N<sub>8</sub>Na<sub>2</sub> requires 1043.53520 (monoisotopic mass). [α]<sub>D</sub><sup>20</sup>: –80.5 (c 1.0, CHCl<sub>3</sub>).

**2,8,14,20-Tetrakis(D-valyl-D-leucinamido)resorc[4]arene Benzyl Ester (10b).** (+)-10b was obtained as described for (–)-10a, starting from tetracarboxylic acid chloride 3 and dipeptide benzyl ester

6b. Pale yellow powder. 65% overall yield. <sup>1</sup>H NMR, <sup>13</sup>C NMR, and ESI-HRMS data are coincident with those reported for (–)-10a. [α]<sub>D</sub><sup>20</sup>: +79.4 (c 1.0, CHCl<sub>3</sub>).

**2,8,14,20-Tetrakis(L-leucyl-L-valinamido)resorc[4]arene Benzyl Ester (11a).** (–)-11a was obtained as described for (–)-10a, starting from tetracarboxylic acid chloride 3 and dipeptide benzyl ester 9a. Pale yellow powder. 75% overall yield. Mp: 248–249 °C. <sup>1</sup>H and <sup>13</sup>C NMR signals are reported in the Supporting Information (Tables 1S and 2S). ESI-HRMS (pos): *m/z* found 1043.53549 ([M + 2Na]<sup>2+</sup>), C<sub>116</sub>H<sub>152</sub>O<sub>24</sub>N<sub>8</sub>Na<sub>2</sub> requires 1043.53520 (monoisotopic mass). [α]<sub>D</sub><sup>20</sup>: –76.7 (c 0.3, CHCl<sub>3</sub>).

**2,8,14,20-Tetrakis(D-leucyl-D-valinamido)resorc[4]arene Benzyl Ester (11b).** (+)-11b was obtained as described for (–)-10a, starting from tetracarboxylic acid chloride 3 and dipeptide benzyl ester 9b. Pale yellow. 65% overall yield. <sup>1</sup>H NMR, <sup>13</sup>C NMR, and ESI-HRMS data are coincident with those reported for (–)-11a. [α]<sub>D</sub><sup>20</sup>: +75.9 (c 1.0, CHCl<sub>3</sub>).

**2,8,14,20-Tetrakis(L-valyl-L-aspartic acid amido)resorc[4]arene Benzyl Ester (16a).** (–)-16a was obtained as described for (–)-10a, starting from tetracarboxylic acid chloride 3 and dipeptide benzyl ester 15a. Pale yellow powder. 54% overall yield. Mp: 218–219 °C. <sup>1</sup>H and <sup>13</sup>C NMR signals are reported in the Supporting Information (Table 3S). ESI-HRMS (pos): *m/z* found 1228.01773 ([M + 2Na]<sup>2+</sup>), C<sub>136</sub>H<sub>152</sub>O<sub>32</sub>N<sub>8</sub>Na<sub>2</sub> requires 1228.01647 (monoisotopic mass). [α]<sub>D</sub><sup>20</sup>: –35.7 (c 0.5, MeOH).

**2,8,14,20-Tetrakis(D-valyl-D-aspartic acid amido)resorc[4]arene Benzyl Ester (16b).** (+)-16b was obtained as described for (–)-10a, starting from tetracarboxylic acid chloride 3 and dipeptide benzyl ester 15b. Pale yellow powder. 56% overall yield. <sup>1</sup>H NMR, <sup>13</sup>C NMR, and ESI-HRMS data are coincident with those reported for (–)-16a. [α]<sub>D</sub><sup>20</sup>: +35.9 (c 0.5, MeOH).

**General Procedure for Pd/C Hydrogenation of Resorc[4]arene Benzyl Esters to Resorc[4]arene Free Acids 12a,b, 13a,b, and 17a,b.** After two vacuum/nitrogen cycles to replace air inside the reaction tube, a mixture of the proper resorc[4]arene benzyl ester (0.05 mmol) and 10% Pd/C (70 mg) in absolute EtOH (4 mL) and dry THF (4 mL) was vigorously stirred at room temperature under 1 atm of hydrogen for 24 h. The reaction mixture was filtered using a membrane filter (Millipore, Millex-LH, 0.45 μm), and the filtrate was concentrated to provide the product, which was dissolved twice in ethyl acetate to remove residual EtOH. The ethyl acetate solution was finally dried under high vacuum at 25 °C, to give resorc[4]arene free acids 12a,b, 13a,b, and 17a,b in quantitative yields.

**2,8,14,20-Tetrakis(L-valyl-L-leucinamido)resorc[4]arene-carboxylic Acid (12a).** (–)-12a was obtained by Pd/C hydrogenation of (–)-10a. Mp: 212–213 °C. <sup>1</sup>H and <sup>13</sup>C NMR signals are reported in the Supporting Information (Tables 1S and 2S). ESI-HRMS (neg): *m/z* found 566.62079 ([M – 4H + Na]<sup>3–</sup>), C<sub>88</sub>H<sub>124</sub>O<sub>24</sub>N<sub>8</sub>Na requires 566.62142 (monoisotopic mass). [α]<sub>D</sub><sup>20</sup>: –55.5 (c 1.0, MeOH). Enantiomeric excess (ee, %) of (–)-12a, checked by enantioselective HPLC, was in the 95–97% range.

**2,8,14,20-Tetrakis(D-valyl-D-leucinamido)resorc[4]arene-carboxylic Acid (12b).** (+)-12b was obtained by Pd/C hydrogenation of (+)-10b. <sup>1</sup>H NMR, <sup>13</sup>C NMR, and ESI-HRMS data are coincident with those reported for (–)-12a. [α]<sub>D</sub><sup>20</sup>: +52.5 (c 1.0, MeOH).

**2,8,14,20-Tetrakis(L-leucyl-L-valinamido)resorc[4]arene-carboxylic Acid (13a).** (–)-13a was obtained by Pd/C hydrogenation of (–)-11a. Mp: 135–136 °C. <sup>1</sup>H and <sup>13</sup>C NMR signals are reported in the Supporting Information (Tables 1S and 2S). ESI-HRMS (neg): *m/z* found 566.62026 ([M – 4H + Na]<sup>3–</sup>), C<sub>88</sub>H<sub>124</sub>O<sub>24</sub>N<sub>8</sub>Na requires 566.62142 (monoisotopic mass). [α]<sub>D</sub><sup>20</sup>: –49.2 (c 0.6, MeOH). Enantiomeric excess (ee, %) of (–)-13a, checked by enantioselective HPLC, was in the 95–97% range.

**2,8,14,20-Tetrakis(D-leucyl-D-valinamido)resorc[4]arene-carboxylic Acid (13b).** (+)-13b was obtained by Pd/C hydrogenation of (+)-11b.  $^1\text{H}$  NMR,  $^{13}\text{C}$  NMR, and ESI-HRMS data are coincident with those reported for (–)-13a.  $[\alpha]_{\text{D}}^{20}$ : +46.3 (*c* 0.7, MeOH).

**2,8,14,20-Tetrakis(L-valyl-L-aspartic acid amido) resorc[4]arene-carboxylic Acid (17a).** (–)-17a was obtained by Pd/C hydrogenation of (–)-16a. Mp: 201–202 °C dec.  $^1\text{H}$  and  $^{13}\text{C}$  NMR signals are reported in the Supporting Information (Table 3S). ESI-HRMS (neg): *m/z* found 843.33097 ( $[\text{M} - 2\text{H}]^{2-}$ ),  $\text{C}_{80}\text{H}_{102}\text{O}_{32}\text{N}_8$  requires 843.33056 (monoisotopic mass).  $[\alpha]_{\text{D}}^{20}$ : –18.3 (*c* 0.1, MeOH).

**2,8,14,20-Tetrakis(D-valyl-D-aspartic acid amido)resorc[4]arene-carboxylic Acid (17b).** (+)-17b was obtained by Pd/C hydrogenation of (+)-16b.  $^1\text{H}$  NMR,  $^{13}\text{C}$  NMR, and ESI-HRMS data are coincident with those reported for (–)-17a.  $[\alpha]_{\text{D}}^{20}$ : +17.7 (*c* 0.1, MeOH).

#### Ultraviolet (UV) and Circular Dichroism (CD) Experiments.

UV and CD spectra of receptors **12** and **13** in TRIS buffer 0.1 M at pH 7.4 ( $4.0 \times 10^{-5}$  M) were obtained using a quartz cuvette with a 1 cm path length at a constant temperature of 25 °C. Eight scans were taken for each sample at 0.2 nm intervals from 190 to 320 nm, at a rate of 20 nm/min. Binding experiments of receptors (–)-12a and (+)-12b with HSA were performed using a double sector quartz cuvette with a 0.9 cm path length, at a constant temperature of 25 °C. Three averaged scans for each CD spectrum were taken at 0.2 nm intervals from 190 to 320 nm, at a rate of 20 nm/min. In these experiments, all samples were dissolved in 0.005 M sodium phosphate buffer (pH = 7.4) at the same concentration ( $5 \times 10^{-6}$  M). The spectra of receptors (–)-12a and (+)-12b alone were subtracted from the spectra of receptors (–)-12a and (+)-12b and HSA, to give difference spectra of receptors (–)-12a and (+)-12b in the presence of HSA (Figure 5).

**Enantioselective HPLC of Peptidoresorc[4]arenes 12 and 13.** Enantioselective HPLC separations were performed on a CHIRALPAK QN-AX (8S,9R) stainless steel column (250 × 4.0 mm i.d.). A mixture of acetonitrile–18 mM ammonium acetate (90:10) was used as the mobile phase. The pH of this mixture (apparent pH) was adjusted to 8.2 by adding HPLC-grade glacial acetic acid. Flow rate: 1.0 mL/min; UV detection at 284 nm. Retention (*k'*) and enantioselectivity ( $\alpha$ ) factors obtained were the following: for peptidoresorc[4]arene **12**,  $k'_L = 2.75$  (corresponding to **12a**);  $k'_D = 3.27$  (corresponding to **12b**);  $\alpha = 1.19$ . For peptidoresorc[4]arene **13**,  $k'_D = 3.13$  (corresponding to **13a**);  $k'_D = 3.98$  (corresponding to **13b**);  $\alpha = 1.27$ . Enantiomeric excesses (ee, %) were in the 95–97% range.

**Gel Electrophoresis.** Agarose gels were prepared in 0.005 M sodium phosphate buffer (pH = 6.0) at a 1% final agarose concentration, the buffer being the mobile phase. Appropriately sized wells (40  $\mu\text{L}$  volume) were formed by placing a comb in the middle of the gel. A ChT  $2 \times 10^{-4}$  M stock solution in 0.005 M sodium phosphate buffer (pH = 7.4) was used to prepare individual samples (30  $\mu\text{L}$ ) of the appropriate ChT/receptor (+)-12b ratio. After a 90 min incubation period at room temperature, 8  $\mu\text{L}$  of 33% glycerol containing tracking dye (bromophenol blue) were added, and a constant voltage (70 V) was applied for approximately 1 h to run the electrophoresis. At the end, the gel was placed in a staining solution (0.5% Coomassie Blue, 40% methanol, 10% acetic acid in water) for 1 h, followed by extensive destaining (40% methanol, 10% acetic acid aqueous solution) until the protein bands became evident.

**General Conditions for Enzymatic Activity Assay.** All experiments were performed in 0.005 M sodium phosphate buffer (pH = 7.4). All solutions were kept at 25 °C during incubation periods and the kinetic analysis. The desired concentrations of the different receptors were achieved by adding a proper quantity of stock solutions in 2-methoxyethanol (for **10**, **12** and **13**) or DMSO (for **16** and **17**) to 1 mL of the phosphate buffer solution of ChT ( $4.0 \times 10^{-8}$  M). ChT and different concentrations of the receptors were kept at 25 °C for a fixed

preincubation period, and then 20  $\mu\text{L}$  of a stock solution of Suc-AAPF-pNA in 2-methoxyethanol were added to reach a final substrate concentration of  $1 \times 10^{-4}$  M. Enzymatic hydrolysis was followed by monitoring *p*-nitroaniline formation at 405 nm for 1 min. The assays were performed in triplicate, and the averages are reported in Table 2 (SD < 3%). The activity of the native ChT (control) was taken to be 100%, and from this value the residual enzymatic activity (%) was calculated.

**Kinetic assay.** ChT activity was measured using Suc-AAPF-pNA as substrate in the absence or presence of (+)-12b or (–)-16a inhibitors, under identical conditions as activity assay. The reaction mixture contained three fixed Suc-AAPF-pNA concentrations (10  $\mu\text{M}$ , 100  $\mu\text{M}$ , and 1000  $\mu\text{M}$ ) with inhibitors concentrations equal to 0, 4, 20, and 40  $\mu\text{M}$  for (+)-12b and 0, 0.4, 1, and 2  $\mu\text{M}$  for (–)-16a.

**Statistical Analysis.** All assays were run in triplicate. Graphs were plotted using Microcal Origin software, version 6.0. Values of the slopes and intercepts were obtained by the linear regression analysis using the same software.  $K_i$  is given as the mean  $\pm$  SD of three values calculated by using the Dixon plots at three different substrate concentrations. Values of  $V_{\text{max}}$  and  $K_m$  were recovered by nonlinear regression analysis based on the Michaelis–Menten equation ( $R^2 = 0.99872$ ).

**Docking Analysis.** The input conformation for receptor (+)-12b was generated by a conformational search carried out with the Macro-Model/Maestro software package (Schrödinger)<sup>20</sup> equipped with Amber\* force field.<sup>21</sup> The search was performed on the rotatable bonds of the four dipeptide side chains of the molecule, which were moved in 3D space with the aim of locating a reliable local minimum energy geometry.<sup>22</sup> In this work, the default settings of Monte Carlo Multiple Minimum search protocol were left unchanged. Analysis of possible binding areas of (+)-12b on the surface of ChT was then carried out by using the program AutoDock 4.0.<sup>18</sup> Further details are given in the Supporting Information.

## ■ ASSOCIATED CONTENT

**S Supporting Information.**  $^1\text{H}$  and  $^{13}\text{C}$  NMR signals of peptidoresorc[4]arenes **10–13** and **16–17**. Structure of the CHIRALPAK QN-AX (8S,9R) chiral stationary phase. Dose-responsive inhibition plots of ChT by (+)-12b and by (–)-16a. ESI-HRMS spectra of peptidoresorc[4]arenes (–)-10a, (–)-11a, (–)-12a, (–)-13a, (–)-16a, and (–)-17a.  $^1\text{H}$  and  $^{13}\text{C}$  NMR spectra of peptidoresorc[4]arenes (+)-10b, (–)-11a, (+)-12b, (–)-13a, (–)-16a, and (+)-17b. Docking analysis and clustering of focused docking experiment. This material is available free of charge via the Internet at <http://pubs.acs.org>.

## ■ AUTHOR INFORMATION

### Corresponding Author

\* Tel.: +390649912781. Fax: +390649912780. E-mail: bruno.botta@uniroma1.it.

### Present Addresses

<sup>||</sup> Department of Molecular Biology, The Scripps Research Institute, La Jolla, California 92037-1000

## ■ ACKNOWLEDGMENT

We acknowledge financial support from FIRB, grant no. RBPR05NWWC\_006, Sapienza Università di Roma, Italy (Funds for Selected Research Topics 2008–2010) and Fondazione Roma (Roma, Italy). This work was partially supported by the “Istituto Pasteur–Fondazione Cenci Bolognetti”, Sapienza Università di Roma, Italy. We gratefully acknowledge Professor F. Gasparrini

(Sapienza Università di Roma, Italy) for assistance with enantioselective HPLC analysis of peptidioresorcin[4]arenes **12** and **13** and for helpful discussions.

## REFERENCES

- (1) (a) Jones, S.; Thornton, J. M. *Proc. Natl. Acad. Sci. U.S.A.* **1996**, *93*, 13–20. (b) Guo, Z.; Zhou, D.; Schultz, P. G. *Science* **2000**, *288*, 2042–2045. (c) Berg, T. *Angew. Chem., Int. Ed.* **2003**, *42*, 2462–2481. (d) Arkin, M. R.; Wells, J. A. *Nat. Rev. Drug Discovery* **2004**, *3*, 301–317.
- (2) (a) Fletcher, S.; Hamilton, A. D. *Curr. Opin. Chem. Biol.* **2005**, *9*, 632–638. (b) Fletcher, S.; Hamilton, A. D. *J. R. Soc., Interface* **2006**, *3*, 215–233.
- (3) Hoffmann, A. S. J. *Biomed. Mater. Res.* **2000**, *52*, 577–586.
- (4) (a) Zutshi, R.; Brichner, M.; Chmielewsky, J. *Curr. Opin. Chem. Biol.* **1998**, *2*, 62–66. (b) Pecuh, M. W.; Hamilton, A. D. *Chem. Rev.* **2000**, *100*, 2479–2494. (c) Yin, H.; Hamilton, A. D. *Angew. Chem., Int. Ed.* **2005**, *44*, 4130–4163. (d) Spring, K. L.; Hamilton, A. D. *Bioorg. Med. Chem. Lett.* **2005**, *15*, 3908–3911. (e) Fletcher, S.; Hamilton, A. D. *Curr. Top. Med. Chem.* **2007**, *7*, 922–927.
- (5) (a) Orner, B. P.; Ernst, J. M.; Hamilton, A. D. *J. Am. Chem. Soc.* **2001**, *123*, 5382–5383. (b) Okhanda, J.; Lockman, J. W.; Kothare, M. A.; Qian, Y.; Blaskovich, M. A.; Sebt, S. M.; Hamilton, A. D. *J. Med. Chem.* **2002**, *45*, 177–178. (c) Yin, H.; Hamilton, A. D. *Bioorg. Med. Chem. Lett.* **2004**, *14*, 1375–1379. (d) Yin, H.; Lee, G.-I.; Sedey, K. A.; Rodriguez, J. M.; Wang, H.-G.; Sebt, S. M.; Hamilton, A. D. *J. Am. Chem. Soc.* **2005**, *127*, 5463–5468. (e) Yin, H.; Lee, G. I.; Sedey, K.; Kutzi, O.; Park, H. S.; Orner, B. P.; Ernst, J. M.; Wang, G. H.; Sebt, S. M.; Hamilton, A. D. *J. Am. Chem. Soc.* **2005**, *127*, 10191–10196. (f) Saraogi, I.; Hamilton, A. D. *Biochem. Soc. Trans.* **2008**, *36*, 1414–1417.
- (6) (a) Ghosh, I.; Chmielewsky, J. *Chem. Biol.* **1998**, *5*, 439–445. (b) Schramm, H. J.; de Rosny, B.; Reboud-Ravaux, M.; Buttner, J.; Dich, A.; Schramm, W. *Biol. Chem.* **1999**, *380*, 593–596. (c) Strong, L. E.; Kiessling, L. L. *J. Am. Chem. Soc.* **1999**, *121*, 6193–6196. (d) Kiessling, L. L.; Gestwicki, J. E.; Strong, L. E. *Curr. Opin. Chem. Biol.* **2000**, *4*, 696–703. (e) Sandanaraj, B. S.; Vutukuri, D. R.; Simard, J. M.; Klaikherd, A.; Hong, R.; Rotello, V. M.; Thayumanavan, S. *J. Am. Chem. Soc.* **2005**, *127*, 10693–10698.
- (7) (a) Fischer, N. O.; McIntosh, C. M.; Simard, J. M.; Rotello, V. M. *Proc. Natl. Acad. Sci. U.S.A.* **2002**, *99*, 5018–5023. (b) Hong, R.; Fischer, N. O.; Verma, A.; Goodman, C. M.; Emrick, T.; Rotello, V. M. *J. Am. Chem. Soc.* **2004**, *126*, 739–743. (c) Hong, R.; Emrick, T.; Rotello, V. M. *J. Am. Chem. Soc.* **2004**, *126*, 13572–13573. (d) You, C.-C.; De, M.; Han, G.; Rotello, V. M. *J. Am. Chem. Soc.* **2005**, *127*, 12873–12881. (e) Fillon, Y.; Verma, A.; Ghosh, P.; Ermenwein, D.; Rotello, V. M.; Chmielewsky, J. *J. Am. Chem. Soc.* **2007**, *129*, 6676–6677.
- (8) (a) Hayashi, T.; Hitomi, Y.; Ogoshi, H. *J. Am. Chem. Soc.* **1998**, *120*, 4910–4915. (b) Jain, R. K.; Hamilton, A. D. *Org. Lett.* **2000**, *2*, 1721–1723. (c) Aya, T.; Hamilton, A. D. *Bioorg. Med. Chem. Lett.* **2003**, *13*, 2651–2654.
- (9) (a) Lin, Q.; Park, H. S.; Hamuro, Y.; Lee, C. S.; Hamilton, A. D. *Biopolymers* **1998**, *47*, 285–297. (b) Park, H. S.; Lin, Q.; Hamilton, A. D. *J. Am. Chem. Soc.* **1999**, *121*, 8–13. (c) Lin, Q.; Hamilton, A. D. *C. R. Chim.* **2002**, *5*, 441–450. (d) Park, H. S.; Lin, Q.; Hamilton, A. D. *Proc. Natl. Acad. Sci. U.S.A.* **2002**, *99*, 5105–5109. (e) Mecca, T.; Consoli, G. M. L.; Geraci, C.; Cunsolo, F. *Bioorg. Med. Chem. Lett.* **2004**, *14*, 5057–5062. (f) Woscholski, R.; Hailes, H. C.; Numbere, M. G. *PCT Int. Appl. WO 2005023744 A2 20050317*, 2005. (g) Francese, S.; Cozzolino, A.; Caputo, I.; Esposito, C.; Martino, M.; Gaeta, C.; Troisi, F.; Neri, P. *Tetrahedron Lett.* **2005**, *46*, 1611–1615. (h) Mecca, T.; Consoli, G. M. L.; Geraci, C.; La Spina, R.; Cunsolo, F. *Org. Biomol. Chem.* **2006**, *4*, 3763–3768.
- (10) (a) Botta, B.; D'Acquarica, I.; Delle Monache, G.; Subissati, D.; Uccello-Barretta, G.; Mastrini, M.; Nazzi, S.; Speranza, M. *J. Org. Chem.* **2007**, *72*, 9283–9290. (b) Botta, B.; Frascchetti, C.; D'Acquarica, I.; Speranza, M.; Novara, F. R.; Mattay, J.; Matthias, C. L. *J. Phys. Chem. A* **2009**, *113*, 14625–14629. (c) Botta, B.; Delle Monache, G.; Salvatore, P.; Gasparrini, F.; Villani, C.; Botta, M.; Corelli, F.; Tafi, A.; Gacs-Baitz,
- E.; Santini, A.; Carvalho, C. F.; Misiti, D. *J. Org. Chem.* **1997**, *62*, 932–938.
- (11) Hamuro, Y.; Crego Calama, M.; Park, H. S.; Hamilton, A. D. *Angew. Chem., Int. Ed.* **1997**, *36*, 2680–2683.
- (12) Verma, A.; Simard, J.; Rotello, V. M. *Langmuir* **2004**, *20*, 4178–4181.
- (13) Botta, B.; Di Giovanni, M. C.; Delle Monache, G.; De Rosa, M. C.; Gacs-Baitz, E.; Botta, M.; Corelli, F.; Tafi, A.; Santini, A.; Benedetti, E.; Pedone, C.; Misiti, D. *J. Org. Chem.* **1994**, *59*, 1532–1541.
- (14) (a) Schiel, C.; Hembury, G. A.; Borovkov, V. V.; Klaes, M.; Agena, C.; Wada, T.; Grimme, S.; Inoue, Y.; Mattay, J. *J. Org. Chem.* **2006**, *71*, 976–982. (b) Kuberski, B.; Pecul, M.; Szumna, A. *Eur. J. Org. Chem.* **2008**, 3069–3078.
- (15) (a) Armstrong, D. W.; Liu, Y.; Ekborg-Ott, K. H. *Chirality* **1995**, *7*, 474–497. (b) Lämmerhofer, M.; Lindner, W. *J. Chromatogr. A* **1996**, *741*, 33–48. (c) Maier, N. M.; Nicoletti, L.; Lämmerhofer, M.; Lindner, W. *Chirality* **1999**, *11*, 522–528. (d) Mandl, A.; Nicoletti, L.; Lämmerhofer, M.; Lindner, W. *J. Chromatogr. A* **1999**, *858*, 1–11.
- (16) (a) Schellenberger, V.; Braune, K.; Hofmann, H.-J.; Jakubke, H.-D. *Eur. J. Biochem.* **1991**, *199*, 623–636. (b) Hedstrom, L.; Perona, J. J.; Rutted, W. *J. Biochemistry* **1994**, *33*, 8757–8763. (c) Perona, J. J.; Craik, C. S. *J. Biol. Chem.* **1997**, *272*, 29987–29990.
- (17) (a) Dixon, M. *Biochem. J.* **1953**, *55*, 170–171. (b) Ahmad, V. U.; Lodhi, M. A.; Abbas, M. A.; Choudhary, M. I. *Fitoterapia* **2008**, *79*, 505–508.
- (18) Huey, R.; Morris, G. M.; Olson, A. J.; Goodsell, D. S. *J. Comput. Chem.* **2007**, *28*, 1145–1152.
- (19) Lozano, P.; De Diego, T.; Iborra, J. L. *Biotechnol. Prog.* **1996**, *12*, 488–493.
- (20) MacroModel v. 9.5 (Amber\*): Mohamadi, F.; Richards, N. G. J.; Guida, W. C.; Liskamp, R.; Lipton, M.; Caufield, C.; Chang, G.; Hendrickson, T.; Still, W. C. *J. Comput. Chem.* **1990**, *11*, 440–467.
- (21) Botta, B.; Caporuscio, F.; Subissati, D.; Tafi, A.; Botta, M.; Filippi, A.; Speranza, M. *Angew. Chem., Int. Ed.* **2006**, *45*, 2717–2720.
- (22) Botta, B.; D'Acquarica, I.; Nevola, L.; Sacco, F.; Valbuena Lopez, Z.; Zappia, G.; Frascchetti, C.; Speranza, M.; Tafi, A.; Caporuscio, F.; Letzel, M.; Mattay, J. *Eur. J. Org. Chem.* **2007**, 5995–6002.